Hindawi
International Journal of Chemical Engineering
Volume 2022, Article ID 2016388, 12 pages
https://doi.org/10.1155/2022/2016388

Research Article

Study on Susceptibility and Mechanism of Reheat Cracking in Welded Joint of Type 347 Austenitic Stainless Steel

Jianjun Wang and Shurong Yu

Lanzhou University of Technology, Lanzhou 730050, China

Correspondence should be addressed to Jianjun Wang; 273256428@qq.com

Received 8 March 2022; Accepted 28 April 2022; Published 31 May 2022

Academic Editor: Selvaraju Narayanasamy

The reheat cracking susceptibility of welded joints has been evaluated by 900°C high-temperature constant load test and 750°C–900°C high-temperature slow strain rate tensile (SSRT) test on welded joints of TP347 steel, and the influencing factors and mechanism of reheat cracking in welded joints have been further investigated by microcosmic characterization techniques of SEM and EDS, etc. The result shows the critical fracture stress of TP347 steel welded joints at 900°C is 24 MPa, which is much lower than 80% of the high-temperature yield strength of base material, indicating that the reheat crack of the welded joint is highly sensitive at this temperature; the average reduction of area (RoA) of welded joints obtained by 750°C–900°C SSRT test at each temperature is below 20%, which means all welded joints have a reheat cracking susceptibility in this temperature range, and the reheat cracking susceptibility increases with the rising of temperature. Based on study and analysis using microcosmic methods of optical microscope, scanning electron microscope, and energy spectrum analysis, it is found that welded joints of TP347 steel have a high reheat cracking susceptibility because the high temperature accelerates the diffusion of Cr, Nb, and impurity elements to the grain boundary, and a large quantity of carbides and low-melting-point eutectics are collected and precipitated at the grain boundary to reduce the plasticity of the grain boundary. Since there is a high welding residual stress in welded joints, cavities are formed under the action of the stress at a high temperature, and the merging of cavities causes the formation of cracks which extend along the grain boundary.

1. Introduction

The stabilization heat-treated TP347 steel welded joints are susceptible to reheat cracking, and this problem has been plaguing the safe service of pressure pipes in industrial plants [1–8]. This paper describes the high-temperature constant load test at stabilization heat treatment temperature (900°C) and high-temperature SSRT test at 750°C, 800°C, 850°C, and 900°C for welded joints of TP347 steel; evaluates the reheat cracking susceptibility of welded joints; investigates the main factors for the generation of reheat cracking of welded joints; further studies the nucleation and extension of reheat cracking by microcosmic characterization techniques of SEM and EDS, etc.; and reveals the formation mechanism of reheat cracking.

2. Test Material and Test Method

2.1. Test Material. The test material was a TP347 steel pipe of Φ457 mm × 45.24 mm, solution treated and passivated by pickling. See Table 1 for its chemical composition. See Table 2 for its mechanical properties.

2.2. Test Method

2.2.1. Specimen Preparation. The welding specimen was made from a TP347 steel pipe with a size of Φ457 mm × 45.24 mm. As shown in Figure 1, the slope is of VY type (P = 1.0 mm, b = 3.0 mm, α = 65°, β = 12°, h = 1/3 T, T = 45.24 mm). The weld metal is 45.24 mm thick (GTAW: 3 mm; SMAW: 42.24 mm).

Table 1: Chemical composition of test material.

Element	C	Mn	*P*	S	Si	Cr	Ni	Nb
Standard value	≤0.08	≤1.00	≤0.030	≤0.020	≤1.00	17.0–19.0	9.0–13.0	10*C–1.0
Finished product	0.059	0.76	0.030	0.001	0.49	17.20	9.75	0.62

Table 2: Mechanical properties of test material.

Test item	Yield strength ReL/MPa	Tensile strength Rm/MPa	Elongation A/%
Standard value	≥205	≥515	≥25
Measured value	332	617	49

See Table 3 for welding parameters. CHG-347 R Φ2.5 mm welding wire and TS-347 3Φ.2 mm welding rod were used for the test.

The completed welding specimen *M* is shown in Figure 2. After welding, the as-welded condition was maintained, welding specimen *M* was visually checked to find that the weld surface was uniform, the overlap between weld passes of multipass welding was even and grooveless, the transition to base material at weld toe was smooth, and the surface was free of defects such as pore, undercut, and slag inclusion. After the satisfactory visual inspection, the specimen passed RT and PT.

See Figure 3 for the macroscopic metallography of welding specimen *M*. The fusion was good and free of defects of cracking, nonfusion, and pore, etc.

The metallographic structures of the weld zone and heat-affected zone (HAZ) of welding specimen *M* are shown in Figure 4. It can be seen that the weld zone structure features ferrite and austenite. The ferrite dendritic grains are evenly distributed on an austenitic matrix in the radial direction of the pipe; it can be seen that HAZ mainly features an austenite structure. There was no visible growth on austenite grains, and the grain size number could be 5 or higher. There was no large quantity of precipitates or coarsened grains at the grain boundary. A lot of lumpy or dotted line-shaped NbC were seen, and this was the NbC from the base material which was not completely solutionized into the matrix and characterized by distribution in the rolling direction of steel.

2.2.2. Reheat Cracking Constant Load Test. The high-temperature constant load test was conducted to measure the critical fracture stress of the specimen at test temperature [9], i.e., apply a constant load on the welded joint specimen at test temperature, and measure the corresponding fracturing time. A series of tests with different loads were conducted. There are two criteria for the reheat cracking test: cracking and fracture. In this paper, the fracture criterion is used, i.e., when the load is less than a certain value, the specimen will not fracture in a certain period. This load is defined as the critical fracture stress at the test temperature. Under this load, cracking will not occur within the specified heat treatment time. According to pertinent literature [10, 11], for stainless steels containing stabilizing elements Ti or Nb, the reheat cracking susceptibility temperature is around 900°C. In engineering, design documents generally specify a stabilization heat treatment temperature of 900°C ± 25°C for TP347 steel, so a test temperature of 900°C was chosen in this paper.

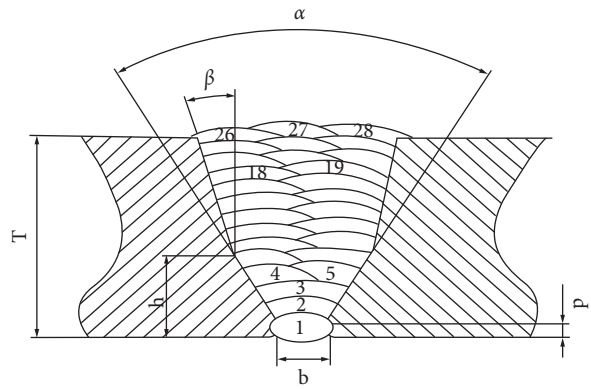

Figure 1: Slope type of welded joint.

High-temperature constant load tests were conducted on 6 mm diameter tensile test specimens of welding specimen *M* under different loads on a high-temperature creep test machine to obtain the fracturing time and critical fracture stress of specimens at 900°C and evaluate the reheat cracking susceptibility of welded joints at 900°C. Typical fractures were observed with a scanning electron microscope, and energy spectrum analysis was conducted on precipitates.

2.2.3. High-Temperature SSRT Test. SSRT test is a test method that evaluates the reheat cracking susceptibility [9]. The test was conducted on a creep test machine. During the test, the specimen was installed on the test machine, heated to the test temperature without applying a load, and maintained at the temperature for 15 min, then pulled at a constant strain rate (5×10^{-4}/s) till it was fractured. When the specimen was cooled to room temperature, its RoA was measured. The reheat cracking susceptibility of the material was estimated according to the RoA [12]. For RoA<5%, it is very susceptible; for 5% < RoA < 10%, it is susceptible; for 10% < RoA < 20%, it is slightly susceptible; and for RoA>20%, it is unsusceptible.

High-temperature SSRT tests were conducted on 6 mm diameter specimens of welding specimen *M* at different temperatures on the high-temperature creep test machine to obtain the RoA of specimens at 750° C, 800° C, 850° C, and 900° C and evaluate the reheat cracking susceptibility of welded joints at different temperatures. Typical fractures

Table 3: Welding parameters.

Specimen no.	Weld layer	Welding method	Polarity	Welding current (A)	Welding voltage (V)	Welding speed ($cm \cdot min^{-1}$)	Heat input ($KJ \cdot cm^{-1}$)
M	1	GTAW	DCSP	100~120	12~13	5.0~5.5	14.4~15.8
	2	SMAW	DCRP	100~110	25~27	9~10	17~19
	Other layers	SMAW	DCRP	100~110	25~27	9~10	17~19

Figure 2: Welding specimen *M*.

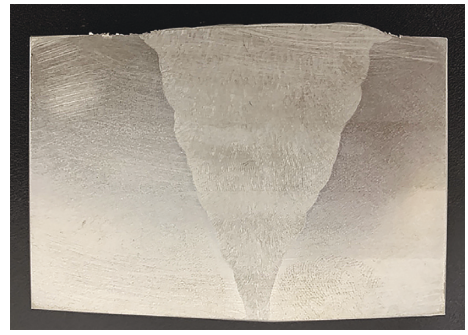

Figure 3: Metallograph of welding specimen M.

were observed with a scanning electron microscope, and energy spectrum analysis was conducted on precipitates.

3. Test Result and Analysis

3.1. High-Temperature Constant Load Test Result and Analysis. See Figure 5 for the specimen fracture appearance in the high-temperature constant load test. See Table 4 and Figure 6 for test result.

All fractures occurred in the weld zone, and this means the strength of the weld zone is lower than that of HAZ and base material. There was no visible necking on the specimen, and this means the plasticity of the welded joint is low.

A load closer to the critical fracture stress is more beneficial to the identification of cracking mechanism, so constant load test specimen fractures M-H5 and M-H6 were selected for SEM and EDS observation and analysis. Figures 7 and 8 show scanning electron micrographs (SEM pictures) of M-H5 and M-H6 constant load test fractures of the specimen at different magnifications. At low magnification (Figure 7), fracture morphology along columnar grains can be seen at both M-H5 and M-H6 fractures. At high magnification (Figure 8), grain boundary cracking along rows of columnar grains can be seen clearly, and there are a lot of precipitates and cavities at the grain boundary. In Figures 9 and 10, it can be seen that the precipitates at the grain boundary are different from intragranular precipitates in form and size. The precipitates at the grain boundary are in a strip shape; too many precipitates are collected and grown and nearly surrounded the grain boundary; intragranular precipitates are mostly in a grain or ellipsoid shape.

Figures 9 and 10 show SEM pictures and EDS analysis of fractures of M-H5 and M-H6 specimens in a constant load test. EDS analysis was conducted on the typical precipitates at the fractures of M-H5 and M-H6 specimens in a constant load test to find out that elements Cr, Nb, O, N, and W were beyond the range of standard chemical composition for the deposited metal of welds. The precipitates were rich in Cr and Nb. According to the analysis, the precipitates should be mainly MC and M23C6. Since the constant load test was conducted under nonvacuum condition, the metal structure contacted the air at a high temperature to generate oxides and nitrides, so the precipitates were rich in elements O and N according to the energy spectrum analysis. However, element W is not supposed to be in TP347 steel and welding material, and it could be an impurity element entrained during steel making.

3.2. High-Temperature SSRT Test Result and Analysis. See Figure 11 for the specimen fracture appearance in the SSRT test. A series of high-temperature SSRT tests were conducted on 6 mm diameter specimens of welding specimen *M* on a high-temperature creep test machine, with two specimens tested at each temperature. See Table 5 and Figure 12 for test result.

Figures 13 and 14 show scanning electron micrographs of fractures of welding specimen *M* in SSRT tests at (a) 750°C, (b) 800°C, (c) 850°C, and (d) 900°C at different magnifications.

At low magnification (Figure 13), it can be seen that fractures of SSRT test specimens are along columnar grains at all test temperatures, without dimples, and are typical ductility dip fractures.

At high magnification (Figure 14), the grain boundary cracking of 900°C SSRT test specimen fractures along rows of columnar grains can be seen more clearly than fractures at other temperatures. The RoA result of SSRT test specimens also decreases with the rising temperature, and this means the reheat cracking susceptibility of TP347 welded joints tends to increase with the rising temperature at 750°C–900°C. It can be seen that the grains at 750°C–850°C

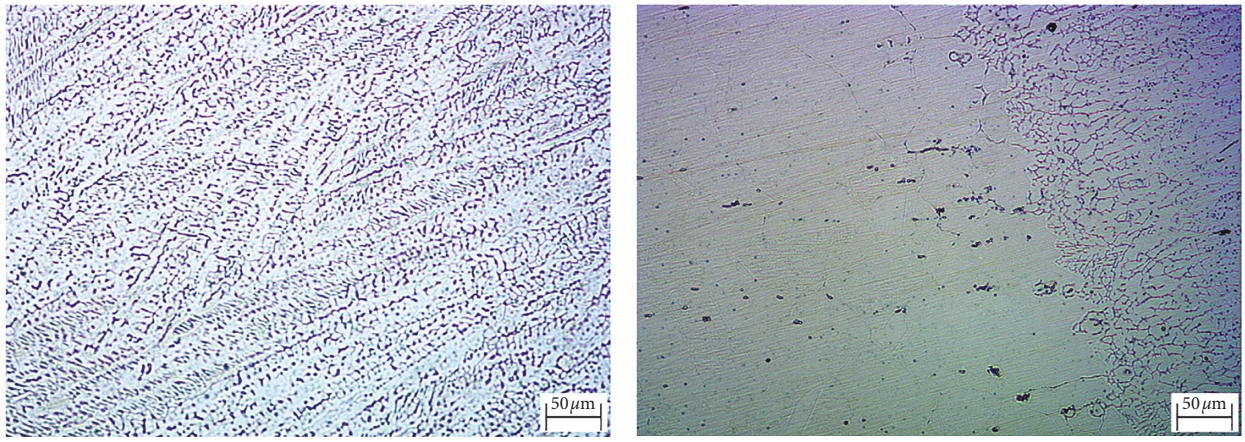

(a) (b)

Figure 4: Metallographic structure of zones of welding specimen *M*. (a) Weld zone, (b) HAZ.

Figure 5: Appearance of fractured constant load test specimen.

Table 4: Welding specimen *M* high-temperature constant load test result.

No	Specimen no	Test load (MPa)	Fracturing time (s)
1	M-H1	76	1167
2	M-H2	50	10012
3	M-H3	40	13856
4	M-H4	35	27997
5	M-H5	30	57551
6	M-H6	28	68865
7	M-H7	26	35658
8	M-H8	24	50550
9	M-H9	23	Not fractured
10	M-H10	20	Not fractured

Note. The reheat cracking critical fracture stress of specimen *M* was 24 MPa, which is much lower than 80% of the high-temperature yield strength of base material, which means the welded joint had a high reheat cracking susceptibility.

SSRT test specimen fractures are in rock candy shape, and some grains are separated to form irregular cavities. A lot of precipitates appear at the grain boundary of fracture. This means the reheat cracking susceptibility is related to the large quantity of precipitates. The higher the temperature, the faster the elements diffuse to the grain boundary, resulting in a large quantity of precipitates appearing at the grain boundary.

In the SEM picture, it can be seen that the precipitates have irregular appearances and sizes (Figure 15). Typical grain boundary precipitates have been selected for EDS analysis (Figure 16) to find out that the precipitates are rich in elements Cr, Nb, Si, and Mn. For this test, TP347 steel has 17.0–19.0 wt% Cr, and TS-347 welding rod has 18.0–21.0 wt% Cr and no more than 1.0 wt% Nb. While the energy spectrum analysis shows the contents of elements Cr and Nb of precipitates are much higher than the standard, this means the precipitates are mainly MC and M23C6.

For this test, TP347 steel has ≤1.0 wt% Mn and ≤1.0 wt% Si, and TS-347 welding rod has 0.5–2.5 wt% Mn and 0.3–0.65 wt% Si. While the energy spectrum analysis shows the contents of elements Mn and Si of precipitates are much higher than the standard, this means a serious segregation occurred to elements Mn and Si at high temperature, and low-melting-point eutectics could be formed to reduce the binding capacity and creep property of grain boundary and facilitate the nucleation and extension of reheat cracking.

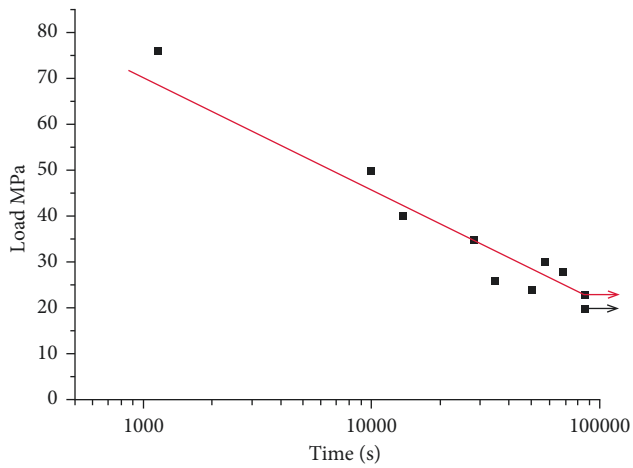

Figure 6: Welding specimen M 900°C high-temperature constant load test result.

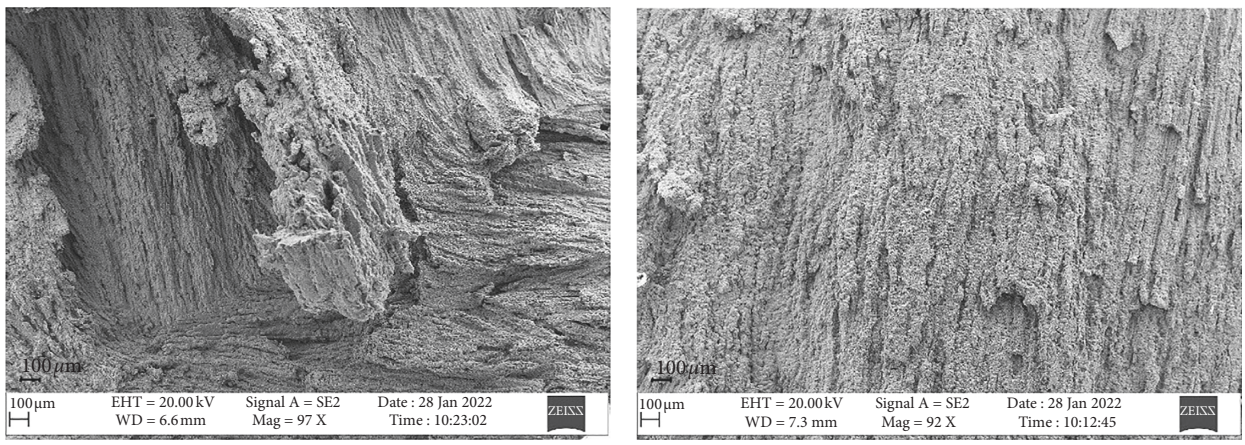

(a) (b)

Figure 7: Low-magnification SEM pictures of fractures at 900°C constant load test. (a) M-H5, (b) M-H6.

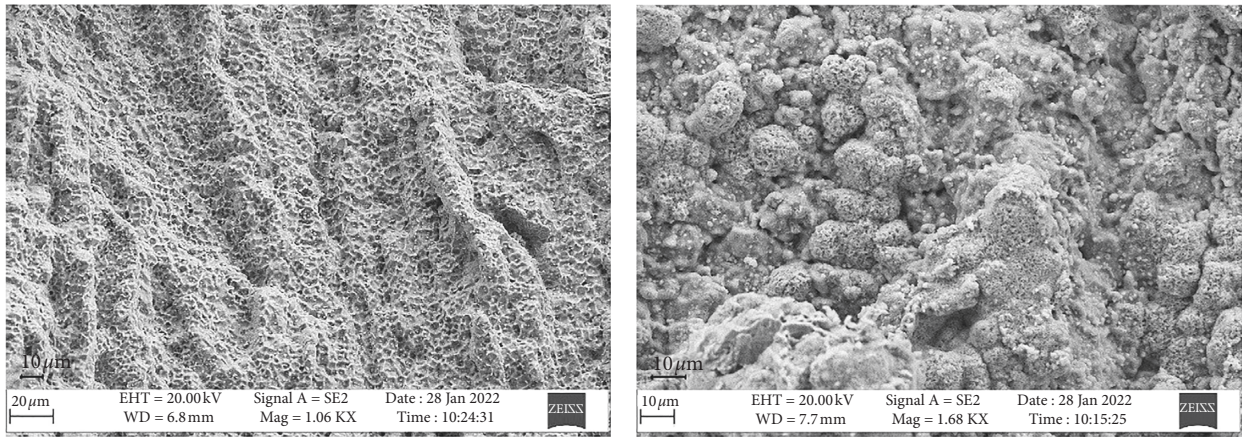

(a) (b)

Figure 8: High-magnification SEM pictures of fractures at 900°C constant load test. (a) M-H5, (b) M-H6.

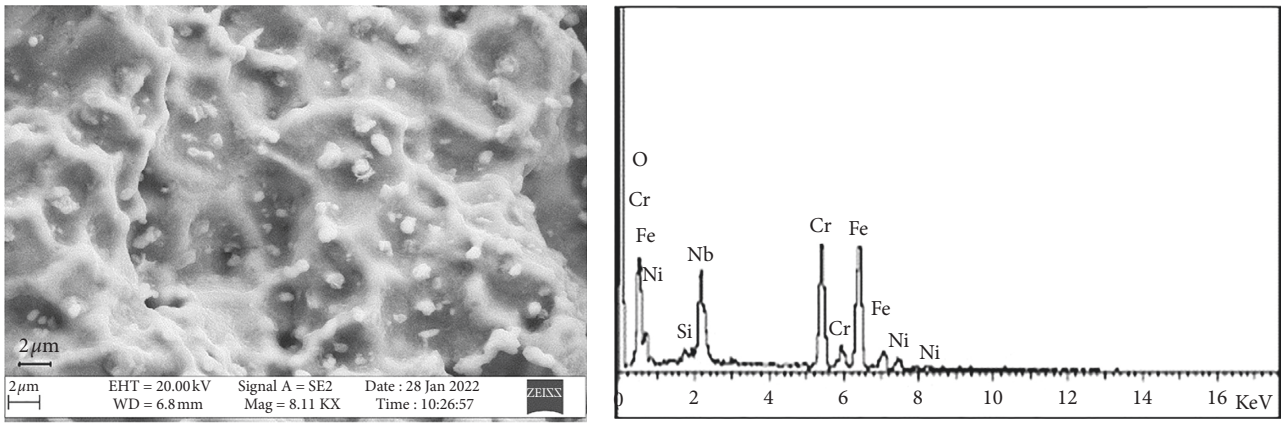

(a) (b)

Figure 9: SEM picture and EDS analysis of M-H5 fracture at 90°C constant load test. (a) SEM picture of precipitates, (b) EDS analysis of precipitates.

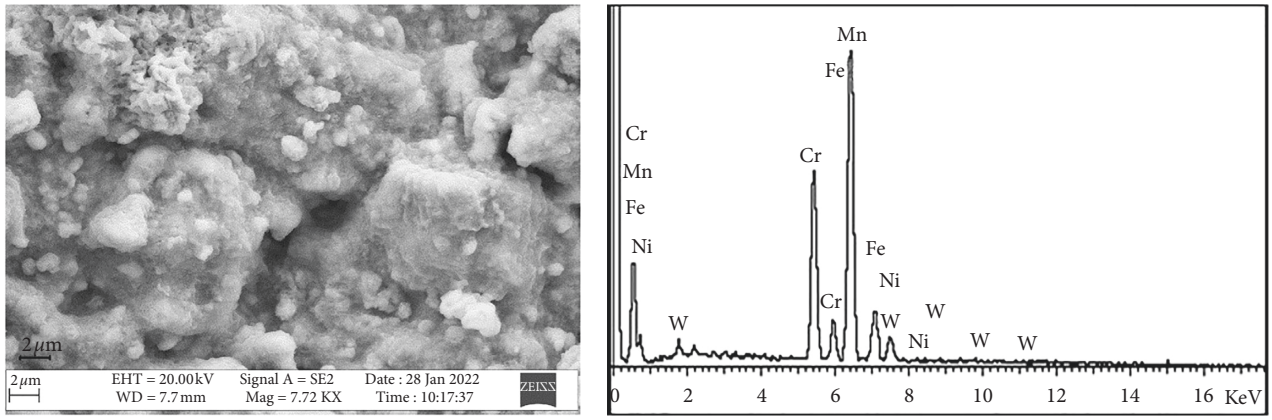

(a) (b)

Figure 10: SEM picture and EDS analysis of M-H6 fracture at 900°C constant load test. (a) SEM picture of precipitates, (b) SEM picture of precipitates.

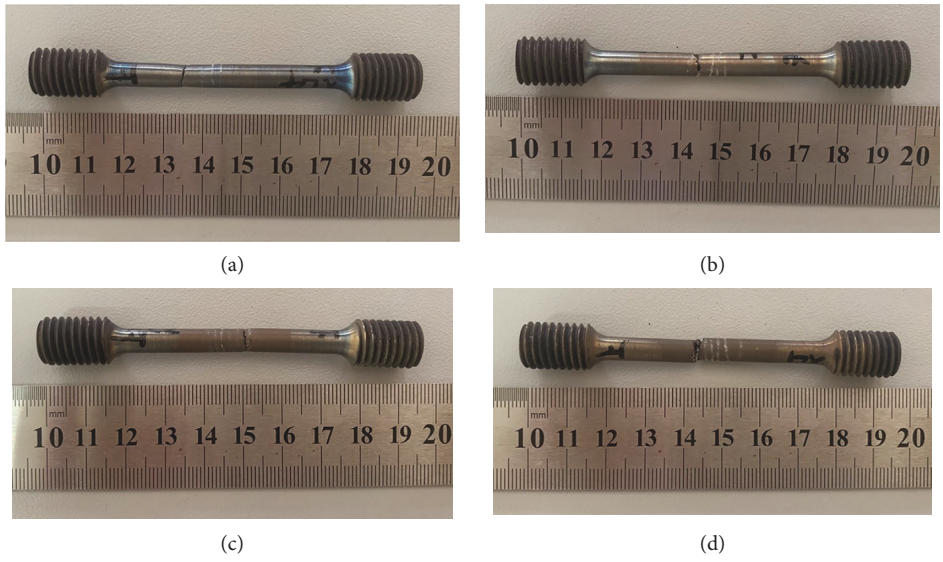

(a) (b)

(c) (d)

Figure 11: Appearance of fractured SSRT test specimens. (a) M-L7 at 750°C, (b) M-L6 at 800°C, (c) M-L4 at 850°C, (d) M-L1 at 900°C.

4. Analysis of Formation Factors and Mechanism of Reheat Cracking

4.1. Formation Factors of Reheat Cracking. The result of high-temperature constant load test and high-temperature SSRT test shows that the reheat cracking susceptibility of thick-wall TP347 steel weld is higher than that of HAZ. At low magnification, it can be seen that all fractures are brittle fractures along the boundary of columnar grains. The essential cause for reheat cracking of TP347 steel welded joints is the nucleation of a large quantity of cavities at grain boundary due to creep ductility dip at a high temperature. Main causes for reheat cracking include the following:

(1) High welding residual stress and stress concentration of thick-wall TP347 steel welded joints. All joints welded with any welding method have welding residual stress, which increases with wall thickness. TP347 steel has a high thermal coefficient of expansion, so it has a high residual stress after welding. At a high temperature, the residual stress in welded joints relaxes, and the grain boundary has a

Table 5: Welding specimen *M* high-temperature SSRT load test result.

No.	Specimen no	Test temperature (°C)	RoA (%)
1	M-L1	900	5.06
2	M-L2	900	7.99
3	M-L3	850	13.13
4	M-L4	850	14.05
5	M-L5	800	24.17
6	M-L6	800	13.66
7	M-L7	750	29.46
8	M-L8	750	16.21

Note. The result shows that at 750°C–900°C, all welded joints have an average RoA less than 20%, which means all welded joints have a reheat cracking susceptibility in this temperature range, and the reheat cracking susceptibility increases with the rising temperature. All fractures occurred at the weld, which means the reheat cracking susceptibility of the weld is higher than that of HAZ and base material.

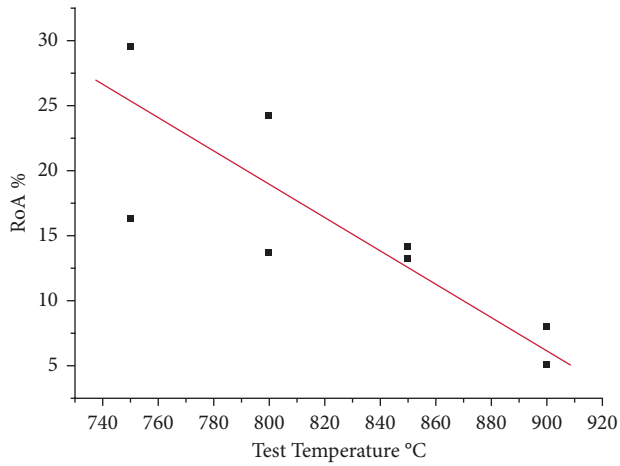

Figure 12: Welding specimen *M* high-temperature SSRT load test result.

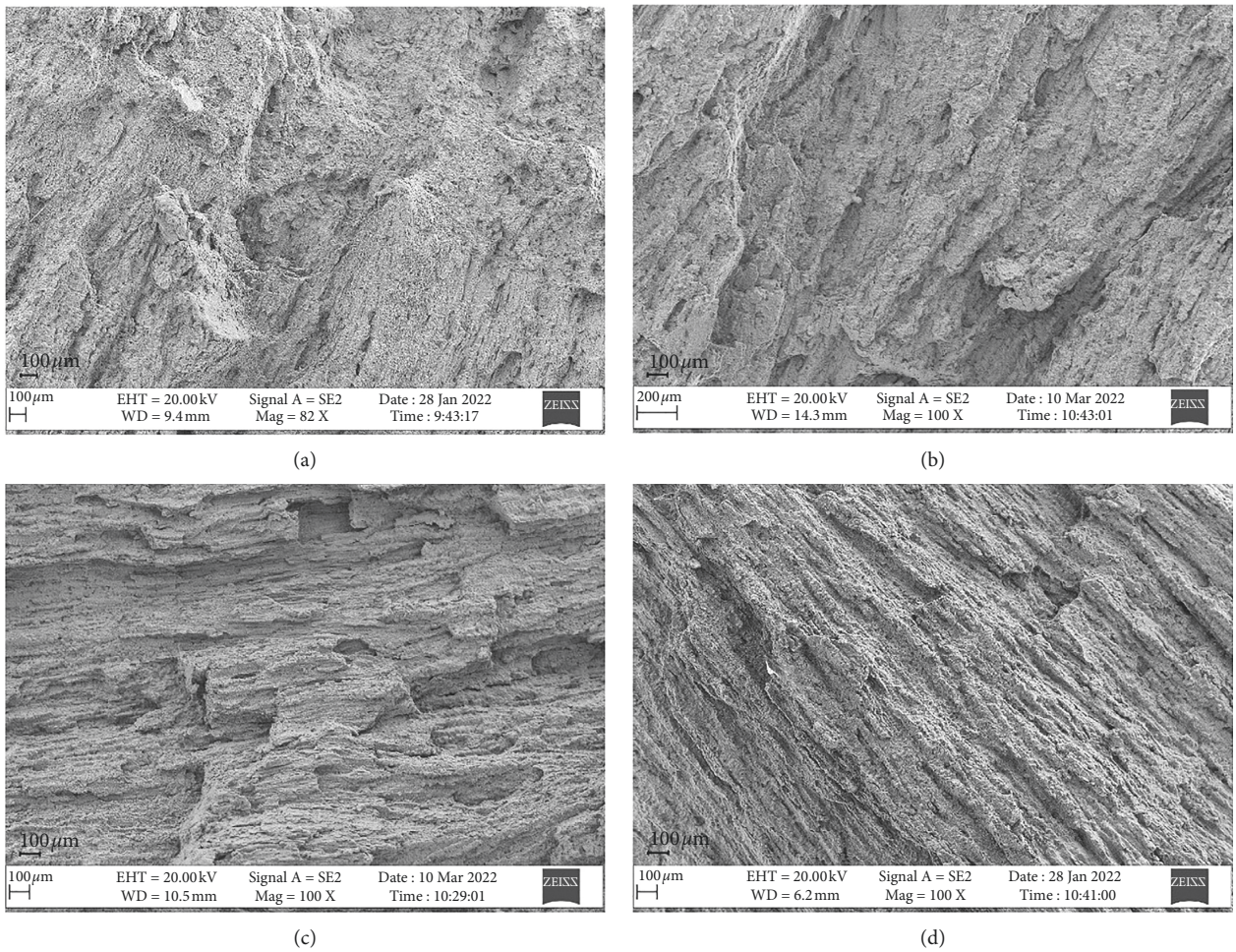

Figure 13: SEM pictures of fractured SSRT test specimens of welded joints. (a) M-L7 at 750°C, (b) M-L6 at 800°C, (c) M-L4 at 850°C, (d) M-L1 at 900°C.

priority in sliding. When the grain boundary plastic deformation exceeds the critical plastic deformability in some stress concentration zones, cracking occurs.

(2) A content of ferrite added to welding material. All fractures occurred at the weld, which means the reheat cracking susceptibility of the weld is higher than that of HAZ. At low magnification, it can be seen that all cracks are along the ferrite dendritic grains or the boundary between ferrite and austenite grains. Energy spectrum analysis shows that the

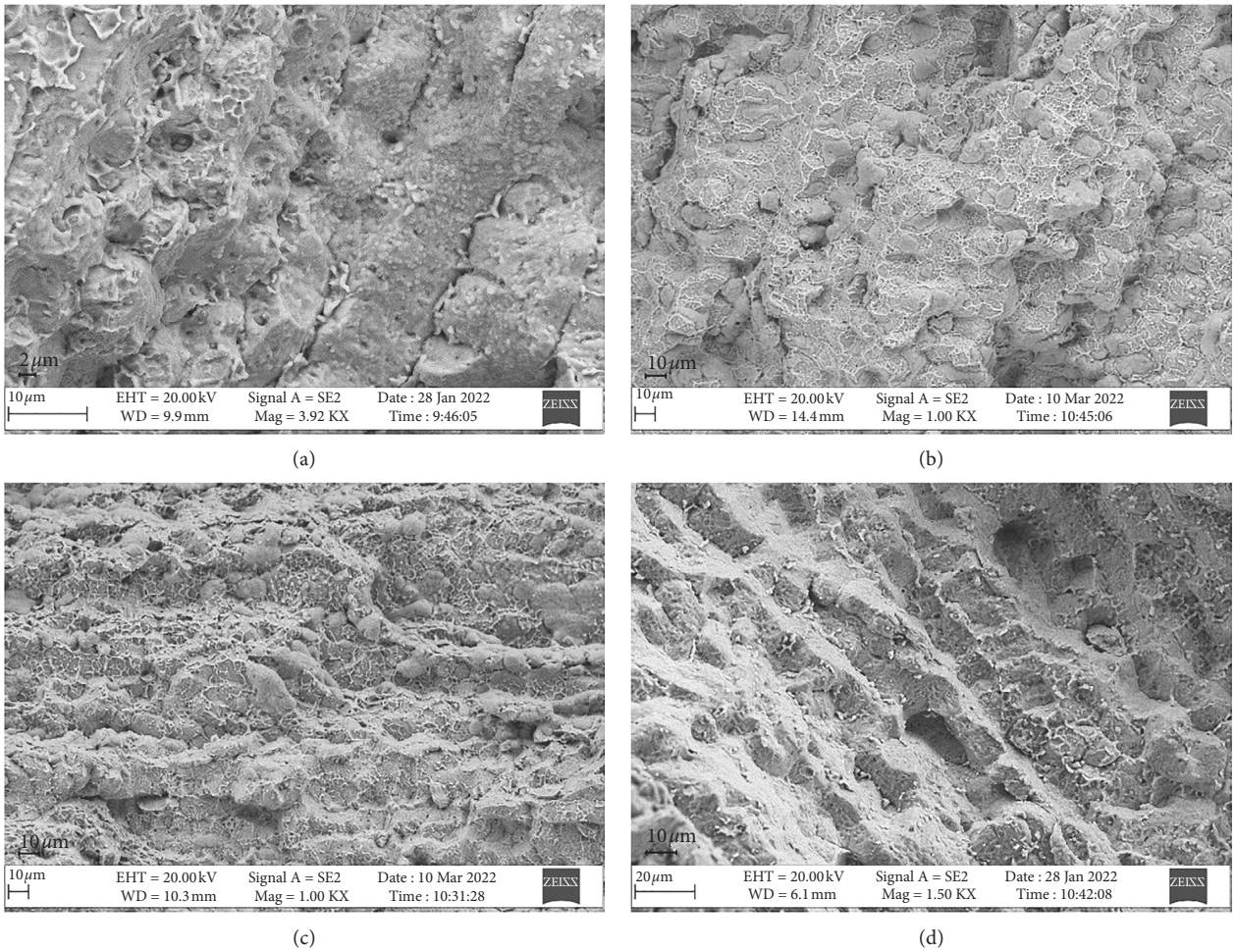

Figure 14: SEM pictures of fractured SSRT test specimens of welded joints. (a) M-L7 at 750°C, (b) M-L6 at 800°C, (c) M-L4 at 850°C, (d) M-L1 at 900°C.

grain boundary is rich in element Cr. With a high content of ferrite, the ferrite is liable to be converted to M23C6 at a high temperature to reduce the plasticity and corrosion resistance of joints.

(3) A large quantity of carbides and low-melting-point eutectics precipitated at the grain boundary. In a microscopic view, it can be seen that all fractures of specimens are along the grain boundary of welds. A large quantity of MC and M23C6 and low-melting-point eutectics containing elements Mn and Si, etc., are precipitated at the grain boundary. At a high temperature, the stress relaxation of welded joints is accompanied by creepage, and too many precipitates reduce the binding capacity and plastic deformability of the grain boundary, resulting in grain boundary cavities, which expand to form cracks under the continuous action of stress.

4.2. Formation Mechanism of Reheat Cracking. A sample was taken from constant load test specimen M-H7, ground, polished, electrochemically corroded with 10% oxalic acid solution, washed, and dried, and then, its weld and HAZ were observed with a scanning electron microscope (Figures 17 and 18).

It can be seen that the weld is significantly different from HAZ in structure. In the weld, there are more ferrite dendritic grains, austenite grains are columnar grains in a strip shape, and there are a large quantity of microcavities at the boundary between ferrites or between ferrites and austenite columnar grains. At high magnification, irregular lumpy precipitates can be seen in cavities and cracking parts (Figure 19(a)). EDS analysis (Figure 19(b)) shows that these precipitates are rich in Nb and must be precipitated NbC. In some zones, microcavities are connected to each other, resulting in crack growth which is in the same direction as dendritic grains. In HAZ, the grains are in an elliptical shape and are obviously bigger than weld grains, but there are no microcavities or cracks in HAZ. This also demonstrates that the reheat cracking susceptibility of the weld is higher than that of HAZ.

A metallographic specimen was taken from the fractured high-temperature constant load specimen M-H7 for observation. As shown in Figure 19, there is a visible grain boundary sliding at the crack. Grain boundary sliding facilitates the formation of cavities. Reheat cracking has a crack form similar to creep fracture, and its cracking

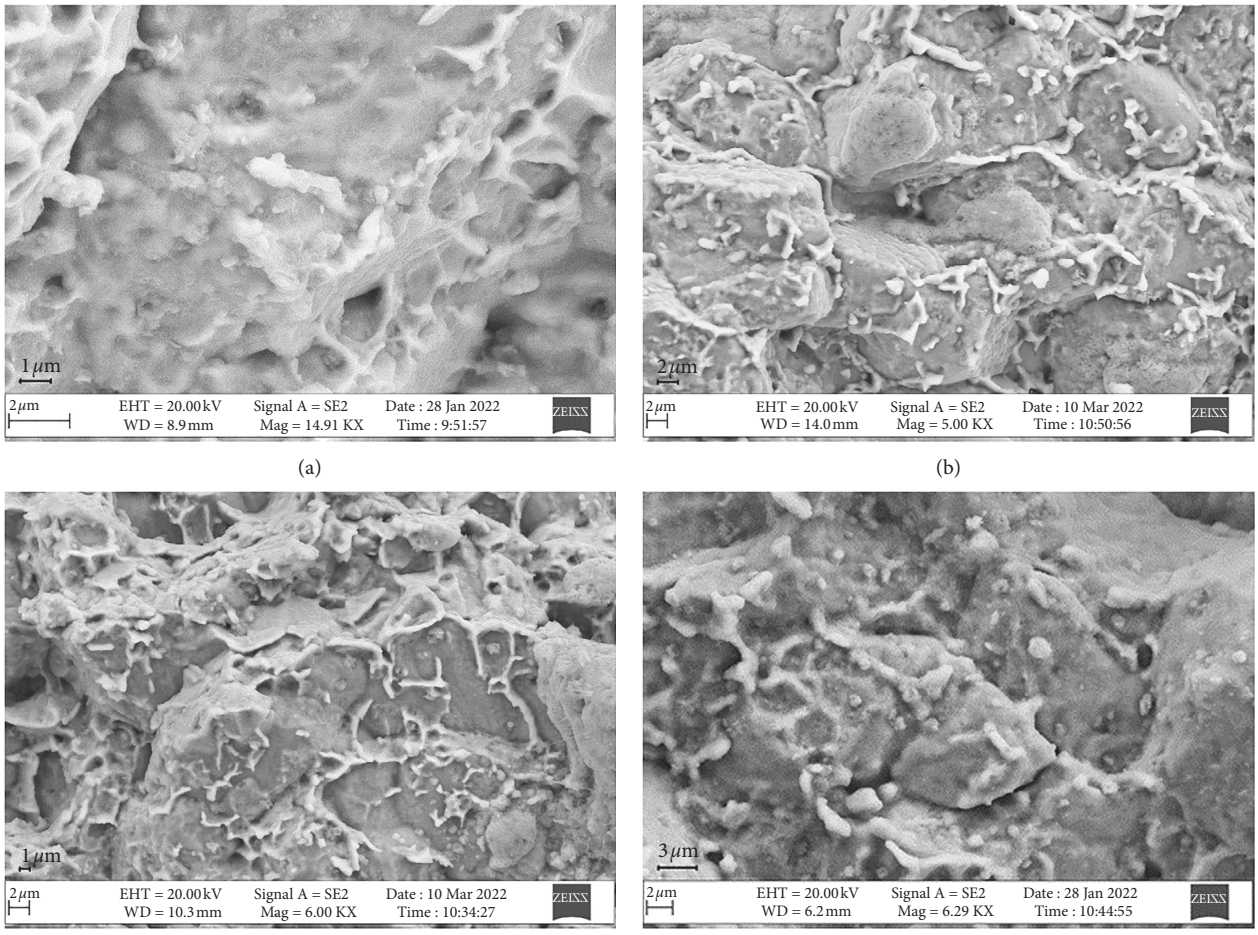

Figure 15: SEM picture of precipitates at SSRT test specimen fracture. (a) M-L7 at 750°C, (b) M-L6 at 800°C, (c) M-L4 at 850°C, (d) M-L1 at 900°C.

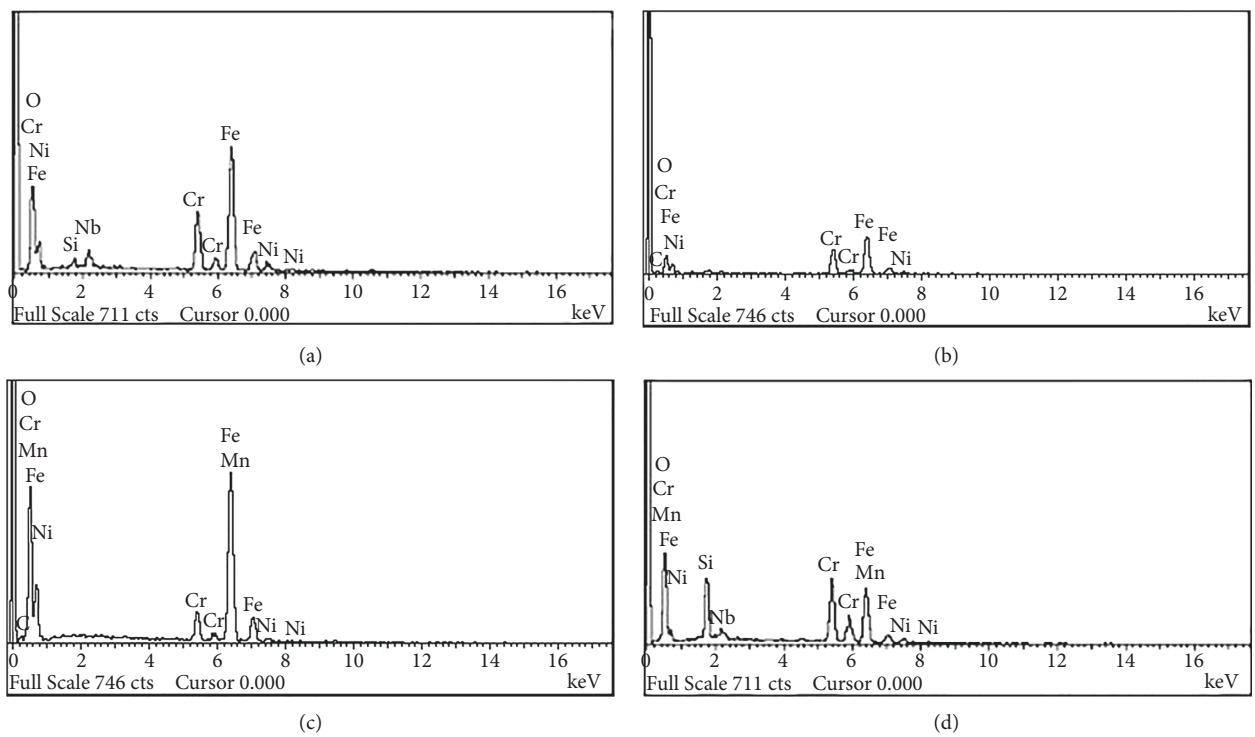

Figure 16: EDS analysis of precipitates at SSRT test specimen fracture. (a) M-L7 at 750°C, (b) M-L6 at 800°C, (c) M-L4 at 850°C, (d) M-L1 at 900°C.

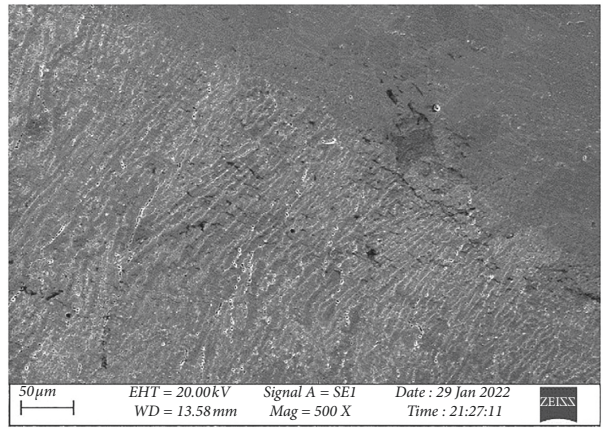

Figure 17: SEM picture of weld and HAZ on high-temperature constant load specimen M-H7.

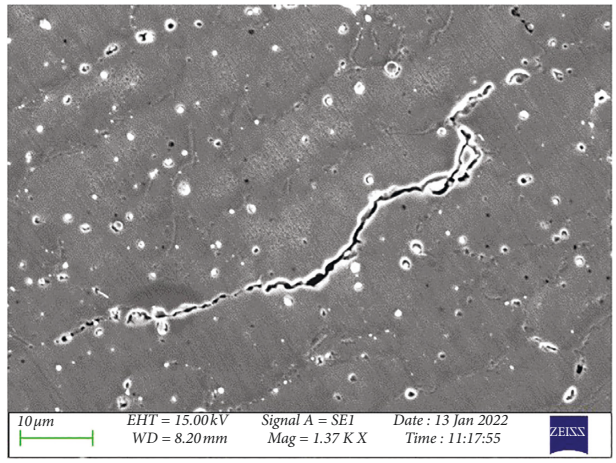

Figure 18: SEM picture of cracking on high-temperature constant load specimen M-H7.

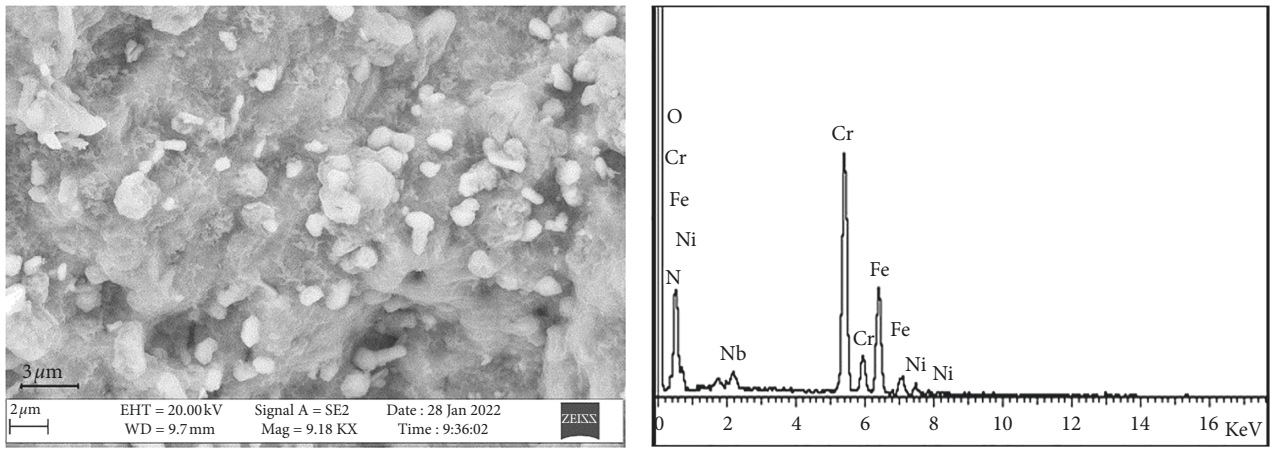

(a) (b)

Figure 19: SEM picture and EDS analysis of M-H7 fracture at 90°C constant load test. (a) SEM picture of precipitates, (b) EDS analysis of precipitates.

mechanism is also the formation and aggregation of cavities. The cracks on the weld extend along the boundary of the original austenite columnar grains.

There is an angle between the direction of the stress applied during the test and the direction of columnar crystals, so the cracks extending along columnar crystals will

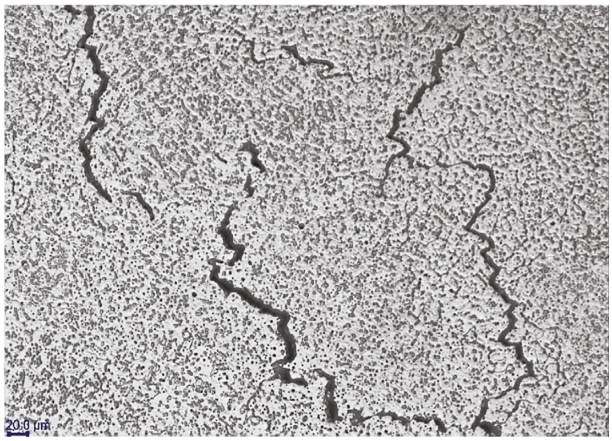

Figure 20: Metallograph of fractured high-temperature constant load specimen M-H7.

intersect. Cracks on one side of columnar crystals are connected to cracks on the other side to form long cracks (Figure 20).

After stabilization heat treatment or high-temperature service, thick-wall TP347 steel pipe welded joints have a high welding residual stress relaxation, leading to grain boundary sliding and formation of cavities. The high temperature accelerates the diffusion of elements C, Cr, Nb, and impurities to cavities and grain boundary. High-temperature SSRT test demonstrates that this diffusion increases with the rising of heat treatment temperature (750°C–900°C), and the corresponding reheat cracking susceptibility increases with the rising of temperature. This indirectly shows that the reheat cracking is mainly resulted from element diffusion causing aggregation and growth of a large quantity of precipitated *M* (C, N) and M23C6 at grain boundary, leading to local stress concentration. When the grain boundary plastic deformation exceeds the critical plastic deformability of the zone, microcavities will be formed, and a large quantity of cavities will merge, leading to crack extension.

5. Conclusion

TP347 steel welded joints were subjected to 900°C high-temperature constant load test and 750°C, 800°C, 850°C, and 900°C SSRT tests, respectively, with main conclusions as follows:

(1) The high-temperature constant load test shows that the critical fracture stress of TP347 steel welded joint at 900°C is 24 MPa. This stress value is much lower than 80% of the high-temperature yield strength of base material, which means welded joints are liable to reheat cracking during stabilization heat treatment at 900°C.

(2) High-temperature SSRT test result shows that TP347 steel welded joints have a reheat cracking susceptibility at 750°C–900°C, and the reheat cracking susceptibility increases with the rising of temperature. Welded joints have the highest reheat cracking susceptibility at 900°C.

(3) Welded joints of TP347 steel have a high reheat cracking susceptibility because the high temperature accelerates the diffusion of Cr, Nb, and impurity elements to the grain boundary, and a large quantity of carbides (MC and M23C6) and low-melting-point eutectics are collected and precipitated at the grain boundary to reduce the plasticity of the grain boundary. In high-temperature condition, the residual stress causes sliding at the grain boundary to generate cavities which merge leading to crack extension.

Data Availability

The data are available on request.

Conflicts of Interest

The authors declare that they have no conflicts of interest.

Acknowledgments

The authors would like to express appreciation to Dr. Shurong Yu for his guidance, support, and patience throughout the study of this research and academic study at Lanzhou University of Technology. With his extensive knowledge and understanding in material science and engineering together with welding engineering, it was a very helpful contribution to understand the problem, develop the investigation techniques, and summarize many ideas in this study.

References

[1] H. Tang and W. S. FuWei, "Causes and treatment measures of cracking in TP347 thick wall pipeline welded joint in hydrogenation unit," *Process Equipment and Piping*, vol. 55, pp. 72–77, 2018.

[2] J. Li, "Heat treatment of 321 and 347 stainless steel welded joints," *Pressure Vessel Technology*, vol. 33, no. 8, pp. 70–74, 2016.

[3] Q. Wang and B. Tian, "Post weld stabilization heat treatment process of TP347 stainless steel," *Electric Welding Machine*, vol. 46, pp. 118–120, 2016.

[4] Z. Luo, X. Dong, and S. Hou, "Material selection and analysis of thick wall stainless steel pipeline in Hydrogenation plant," *Petroleum Refinery Engineering*, vol. 44, no. 12, pp. 37–41, 2014.

[5] Z. Dai, "Heat crack and reheat crack in weld in austenitic steel 347H," *Process Equipment and Piping*, vol. 47, no. 3, pp. 54–58, 2010.

[6] J. Swaminathan, R. Singh, M. K. Gunjan, and B. Mahato, "Sensitization induced stress corrosion failure of AISI 347 stainless steel fractionator furnace tubes," *Engineering Failure Analysis*, vol. 18, no. 8, pp. 2211–2221, 2011.

[7] Z. Liang and Q. Zhao, "Steam oxidation of austenitic heat-resistant steels TP347H and TP347HFG at 650–800°C," *Materials*, vol. 12, no. 4, p. 577, 2019.

[8] H. Bu, M. Ren, and Y. Zhou, "Experimental study of reheat crack on TP321H stainless steel," *Pressure Vessel Technology*, vol. 37, no. 12, pp. 8–14, 2020.

[9] H. Bu, X. Chen, and X. Luo, "Test procedure for reheat cracking susceptibility of welding material used to 2.25Cr-

1 Mo-0.25 V steel," *Pressure Vessel Technology*, vol. 32, no. 10, pp. 1–7, 2015.

[10] P. On and Isaratat, *An Investigation of Reheat Cracking in the Weld Heat Affected Zone of Type 347 Stainless Steel*, The Ohio State University, Columbus, Ohio, 2007.

[11] J. C. Lippoid and D. J. Kotecki, *Welding Metallurgy and Weldability of Stainless Steels*, China Machine Press, Beijing, China, 2008.

[12] American Welding Society, *Welding Handbook*, Maimi, Florida, American Welding Society, 8th edition, 1991.